CHALMERS
UNIVERSITY OF TECHNOLOGY

Performance Analysis of Hybrid 5G-GNSS Localization

Citation for the original published paper (version of record):
Destino, G., Saloranta, J., Seco-Granados, G. et al (2018). Performance Analysis of Hybrid 5G-GNSS Localization. Conference Record - Asilomar Conference on Signals, Systems and Computers: 8-12. http://dx.doi.org/10.1109/ACSSC.2018.8645207

(article starts on next page)

Performance Analysis of Hybrid 5G-GNSS Localization

Giuseppe Destino*§, Jani Saloranta*, Gonzalo Seco-Granados†, and Henk Wymeersch‡
*University of Oulu, Oulu, Finland
†Universitat Autonoma de Barcelona, Barcelona, Spain
‡Chalmers University of Technology, Gothenburg, Sweden
§King's College London, London, United Kingdom
email: {giuseppe.destino, jani.saloranta}@oulu.fi, henkw@chalmers.se, gonzalo.seco@uab.cat

***Abstract*—We consider a novel positioning solution combining millimeter wave (mmW) 5G and Global Navigation Satellite System (GNSS) technologies. The study is carried out theoretically by deriving the Fisher Information Matrix (FIM) of a combined 5G-GNSS positioning system and, subsequently, the position, rotation and clock-bias error lower bounds. We pursue a two-step approach, namely, computing first the FIM for the channel parameters, and then transforming it into the FIM of the position, rotation and clock-bias. The analysis shows advantages of the hybrid positioning in terms of i) localization accuracy, ii) coverage, iii) precise rotation estimation and iv) clock-error estimation. In other words, we demonstrate that a tight coupling of the two technologies can provide mutual benefits.**

I. Introduction

It is well-known that accurate radio-based positioning is the enabler of many location-based services related for instance to safety, intelligent transportation, entertainment, industry automation, robotics and remote operation services [1], [2]. However, Global Navigation Satellite System (GNSS), which is a term that comprises GPS and Galileo among other systems, constitutes still today the only wide-spread reliable solution thanks to its high precision and coverage [3]. In [4], it is shown that also millimeter wave (mmW) 5G technology can be used for accurate positioning, especially in indoor environment where GNSS solutions are not feasible. For this reason positioning has gained interest in 3GPP, searching for a standardized way to improve LTE-techniques using the so-called New Radio (NR) and, potentially, GNSS jointly.

In this paper we study a novel solution combining mmW 5G and GNSS technologies, extending the work in [5], with the objective of improving GNSS coverage and, overall, enabling better localization performance. The study is carried on from a theoretical perspective deriving the Fisher Information Matrix (FIM) [6] of a hybrid 5G-GNSS localization estimation and, subsequently, the position and rotation error lower bound. We pursue a two-step approach, namely, computing first the FIM for the position-related channel parameters and after, the Equivalent Fisher Information Matrix (EFIM) for position and rotation. Also, we look at the UE's clock-bias estimation, which is the enabler for Time-of-Arrival (ToA) estimation.

The reminder of this paper is organized as follows. In Section II we define the 5G-GNSS system model.

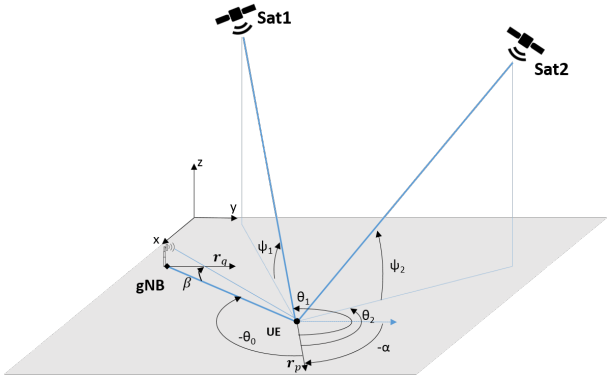

Fig. 1. Transmission links and geometry of the scenario including a 5G station (gNB) at location $\mathbf{q}$ and receiver (UE) at location $\mathbf{p}$ as well as two satellite stations at location $\mathbf{q}_1$ and $\mathbf{q}_2$, respectively. All links are assumed in LOS. The angle α is the rotation of the UE with respect to the gNB heading.

In Sections III and IV, we tackle the 5G-GNSS position-rotation bound by providing the key derivation steps along with numerical results. Finally, in Section V useful insights are drawn.

II. System Model

We consider an hybrid positioning system including GNSS and mmW 5G technology as depicted in Figure 1. More specifically, we assume a UE connected to both a 5G station (gNB) and S satellites. Also, UE is equipped with an antenna array to receive 5G and GNSS signals.

The vector $\mathbf{p} \triangleq [p_x, p_y, p_z]^{\mathrm{T}}$ denotes the location of the UE in the 3-dimensional (3D) space, whereas the vector $\mathbf{q}_i \triangleq [q_{ix}, q_{iy}, q_{iz}]^{\mathrm{T}}$ refers to the 3D coordinate vector of a reference station, with $i = 0$ for the gNB and $i > 0$ for the satellites. We assume $\mathbf{q}_i$ is known, $\forall i$. Also, $\mathbf{q}_0$ is fixed, whereas $\mathbf{q}_i$ with $i > 0$ changes with time, with velocity $\mathbf{v}_i \in \mathbb{R}^3$. Finally, we assume that the direction of the gNB's and UE's antenna boresight is indicated by the 3D orientation vectors $\mathbf{r}_q$ and $\mathbf{r}_p$, respectively. The direction $\mathbf{r}_q$ is known, whereas the relative orientation of $\mathbf{r}_p$ with respect to $\mathbf{r}_q$ can also be represented by the azimuth-elevation pair (α, β), which are unknown parameters to be determined.

The positioning of the UE is based on the joint processing of the received 5G and GNSS signals, respectively, denoted by $\mathbf{y}_0(t)$ and $\mathbf{y}_s(t)$. More specifically, $\mathbf{y}_0(t)$ is given by

$$\mathbf{y}_0(t) = \sqrt{P_g}\mathbf{W}^{\mathrm{H}}\mathbf{H}(a_0,\theta_0,\psi_0,\phi_0,\xi_0,\alpha)\mathbf{F}\mathbf{x}_0(t-\tau_0)e^{j2\pi t f_{d_0}} + \mathbf{W}^{\mathrm{H}}\mathbf{n}(t), \quad (1)$$

where P_g is the transmission power at the gNB, $\mathbf{W} \in \mathbb{C}^{M\times M_b}$ and $\mathbf{F} \in \mathbb{C}^{N\times N_b}$ are the receive and transmit analog-digital hybrid beamforming matrices, f_{d_0} is the Doppler frequency, $\mathbf{x}_0(t) \in \mathbb{C}^{N_b}$ is vector of N_b reference signals transmitted by the 5G station, τ_0 is the path-delay defined as

$$\tau_0 = \varrho_0 - \delta t, \quad (2)$$

where $\varrho_0 \triangleq \|\mathbf{q}_0 - \mathbf{p}\|/c$ is the time-of-flight, c is the speed-of-light, δt is the UE's clock-bias with respect to the GNSS time[1] The $M \times N$ complex channel matrix is given by

$$\mathbf{H}(a_0,\theta_0,\psi_0,\phi_0,\xi_0,\alpha) = a_0\mathbf{a}_{r,0}(\theta_0,\psi_0,\alpha)\mathbf{a}_{t,0}^{\mathrm{H}}(\phi_0,\xi_0), \quad (3)$$

where $a_0 \in \mathbb{C}$ denotes the channel coefficient, α is the rotation[2], θ_0, ψ_0 and ϕ_0, ξ_0 are the azimuth, elevation angles of the angle-of-arrival (AoA) and angle-of-departure (AoD), respectively. The vectors $\mathbf{a}_{r,0}(\cdot) \in \mathbb{C}^M$, $\mathbf{a}_{t,0}(\cdot) \in \mathbb{C}^N$ denote the receive and transmit steering vectors and are computed as,

$$\mathbf{a}_{r,0}(\theta_0,\psi_0,\alpha) \triangleq \exp\left(j\pi\mathbf{R}_u^{\mathrm{T}}\mathbf{\Gamma}^{\mathrm{T}}(\alpha)\boldsymbol{\pi}(\theta_0,\psi_0)\right), \quad (4)$$

$$\mathbf{a}_{t,0}(\phi_0,\xi_0) \triangleq \exp\left(j\pi\mathbf{R}_g^{\mathrm{T}}\boldsymbol{\pi}(\phi_0,\xi_0)\right), \quad (5)$$

where $\boldsymbol{\pi}(a,b)$ is the unit-vector given by

$$\boldsymbol{\pi}(a,b) \triangleq [\cos(b)\cos(a), \cos(b)\sin(a), \sin(b)]^{\mathrm{T}}, \quad (6)$$

$\mathbf{R}_u \in \mathbb{R}^{3\times M}$ (similarly $\mathbf{R}_g \in \mathbb{R}^{3\times N}$) is the antenna element location[3] matrix for the UE (and 5G-station), *i.e.*,

$$\mathbf{R}_u = \begin{bmatrix} 0 & r_{1x} & \cdots & r_{Mx} \\ 0 & r_{1y} & \cdots & r_{My} \\ 0 & r_{1z} & \cdots & r_{Mz} \end{bmatrix}, \quad (7)$$

and, finally, the matrix $\mathbf{\Gamma}(\alpha)$ is the rotation matrix given by

$$\mathbf{\Gamma}(\alpha) = \begin{bmatrix} \cos\alpha & -\sin\alpha & 0 \\ \sin\alpha & \cos\alpha & 0 \\ 0 & 0 & 1 \end{bmatrix}. \quad (8)$$

The received superposition of the GNSS signals is given by

$$\mathbf{y}_s(t) = \mathbf{G}(\boldsymbol{\theta}_s,\boldsymbol{\psi}_s,\alpha)\mathbf{A}_s\mathbf{d}(t,\boldsymbol{\tau}_s,\mathbf{f}_d) + \mathbf{n}_s(t), \quad (9)$$

where $\mathbf{y}_s(t) \in \mathbb{C}^{M_s}$ with M_s as the number of GNSS antenna elements, $\mathbf{A}_s \in \mathbb{C}^{S\times S}$ is a diagonal matrix in which the ii-th element, a_i is the complex amplitude of the received signal transmitted by the i-th satellite, $\boldsymbol{\theta}_s \triangleq [\theta_1,\cdots,\theta_S]$ and $\boldsymbol{\psi}_s \triangleq [\psi_1,\cdots,\psi_S]$ are the azimuth and elevation vectors of the AoA of the impinging satellite signals, the matrix $\mathbf{G}$ is referred to as spatial signature matrix and given by

$$\mathbf{G}(\boldsymbol{\theta}_s,\boldsymbol{\psi}_s,\alpha) \triangleq [\mathbf{a}_{r,s}(\theta_1,\psi_1,\alpha),\cdots,\mathbf{a}_{r,s}(\theta_S,\psi_S,\alpha)], \quad (10)$$

[1]The gNB is assumed perfectly synchronized with the GPS time.

[2]For simplicity, only a rotation around the z-axis is considered, *i.e.*, $\beta = 0$.

[3]Element locations are measured in wavelength unit and with respect to 1-st one (origin).

with

$$\mathbf{a}_{r,s}(\theta_i,\psi_i,\alpha) \triangleq \exp\left(j\pi\mathbf{R}_s^{\mathrm{T}}\mathbf{\Gamma}^{\mathrm{T}}(\alpha)\boldsymbol{\pi}(\theta_i,\psi_i)\right), \quad (11)$$

$\mathbf{R}_s \in \mathbb{R}^{3\times M_s}$ denoting the GNSS antenna element location matrix and $\mathbf{d}(t,\boldsymbol{\tau}_s,\mathbf{f}_d) \in \mathbb{C}^S$ is the vector of delayed Doppler-shifted GNSS signal with $d_i(t)$ given by

$$d_i(t) \triangleq d_i(t,\tau_i,f_{d_i}) = x_i(t-\tau_i)e^{j2\pi f_{d_i}t}, \quad (12)$$

where each $x_i(t)$ is orthogonal to each other, and τ_i is

$$\tau_i = \varrho_i - \delta t, \quad (13)$$

with $\varrho_i \triangleq \|\mathbf{q}_i - \mathbf{p}\|/c$ and f_{d_i} being the time-of-flight and Doppler shift between the UE and the i-th satellite.

III. Position-orientation lower bound analysis

In order to derive the position-orientation error for the hybrid 5G-GNSS positioning system, we compute the 5G-GNSS EFIM as

$$\mathbf{J}^e = \mathbf{J}_0^e + \mathbf{J}_s^e, \quad (14)$$

with $\mathbf{J}_0^e$ and $\mathbf{J}_s^e$ referring to the EFIM for the location parameters $\boldsymbol{\eta} \triangleq [\mathbf{p}^{\mathrm{T}},\alpha,\delta_t]^{\mathrm{T}}$ obtained with the 5G and satellite signals, respectively.

The GNSS EFIM $\mathbf{J}_s^e$ is given by

$$\mathbf{J}_s^e = \sum_{i=1}^{S}\left(\mathbf{J}_{s_i,\eta} - \mathbf{J}_{s,\eta a_i}\mathbf{J}_{s,a_i}^{-1}\mathbf{J}_{s,\eta a_i}^{\mathrm{T}}\right), \quad (15)$$

where

$$\mathbf{J}_{s_i,\eta} = \frac{1}{N_0}\int_0^{T_s}\Re\{\nabla_{\boldsymbol{\eta}}^{\mathrm{H}}\boldsymbol{u}_{s_i}(t,\boldsymbol{\eta},a_i)\nabla_{\boldsymbol{\eta}}\boldsymbol{u}_{s_i}(t,\boldsymbol{\eta},a_i)\}\,\mathrm{d}t, \quad (16)$$

$$\mathbf{J}_{s_i,a_i} = \frac{1}{N_0}\int_0^{T_s}\Re\{\nabla_{a_i}^{\mathrm{H}}\boldsymbol{u}_{s_i}(t,\boldsymbol{\eta},a_i)\nabla_{a_i}\boldsymbol{u}_{s_i}(t,\boldsymbol{\eta},a_i)\}\,\mathrm{d}t, \quad (17)$$

$$\mathbf{J}_{s_i,\eta a_i} = \frac{1}{N_0}\int_0^{T_s}\Re\{\nabla_{\boldsymbol{\eta}}^{\mathrm{H}}\boldsymbol{u}_{s_i}(t,\boldsymbol{\eta},a_i)\nabla_{a_i}\boldsymbol{u}_{s_i}(t,\boldsymbol{\eta},a_i)\}\,\mathrm{d}t, \quad (18)$$

where T_s is the observation time of the GNSS signal, $\boldsymbol{u}_{s_i}(t,\boldsymbol{\eta},a_i)$ is defined as

$$\boldsymbol{u}_{s_i}(t,\boldsymbol{\eta},a_i) \triangleq a_i\tilde{\mathbf{g}}_i(\mathbf{p},\alpha)x_i(t-\tilde{\tau}_i(\mathbf{p}))e^{j2\pi\tilde{f}_i(\mathbf{p},\mathbf{v})t}, \quad (19)$$

where $\tilde{\mathbf{g}}_i(\mathbf{p},\alpha)$, $\tilde{\tau}_i(\mathbf{p})$ and $\tilde{f}_i(\mathbf{p},\mathbf{v})$ indicate a re-parameterization of the i-th column of (10), the i-th path-delay (both measured with 5G and GNSS signals) and the i-th Doppler-frequency as a function of the location and rotation and velocity vector.

Similarly, the 5G-based EFIM is given by

$$\mathbf{J}_0^e = \mathbf{J}_{0,\eta} - \mathbf{J}_{0,\eta a_0}\mathbf{J}_{0,a_0}^{-1}\mathbf{J}_{0,\eta a_0}^{\mathrm{T}}, \quad (20)$$

with $\mathbf{J}_{0,\eta} = \sum_{m=1}^{M_b}\mathbf{J}_{0m,\eta}$, $\mathbf{J}_{0,a_0} = \sum_{m=1}^{M_b}\mathbf{J}_{0m,a_0}$ and $\mathbf{J}_{0,\eta a_0} = \sum_{m=1}^{M_b}\mathbf{J}_{0m,\eta a_0}$ and $\mathbf{J}_{0m,\eta}, \mathbf{J}_{0m,\eta}$ and $\mathbf{J}_{0m,\eta a_0}$ are computed as

in (16), (17) and (18) by replacing T_s with T_g and $\mathbf{u}_{s_i}(t,\boldsymbol{\eta},a_i)$ with

$$u_{0m}(t,\boldsymbol{\eta},a_0)\triangleq\sqrt{P_g}\mathbf{w}_m^{\mathrm{H}}\tilde{\mathbf{H}}(\mathbf{p},\alpha,a_0)\mathbf{F}\mathbf{x}_0(t-\tilde{\tau}_0(\mathbf{p}))e^{j2\pi\tilde{f}_0(\mathbf{p},\mathbf{v})t} \tag{21}$$

where the subscript m refers to the m-th baseband chain, $\tilde{f}_0(\mathbf{p},\mathbf{v})$ and $\tilde{\mathbf{H}}(\mathbf{p},\alpha,a_0)$, are, respectively, a re-parameterization of the 5G-based channel matrix and Doppler frequency as a function of the location and rotation and velocity vector. The re-parameterization is explicited as follows

$$\theta_i = \text{atan}\left(\frac{p_y-q_{iy}}{p_x-q_{ix}}\right)-\pi, \tag{22}$$

$$\phi_0 = \text{atan}\left(\frac{p_y-q_{0y}}{p_x-q_{0x}}\right), \tag{23}$$

$$\psi_i = \text{atan}\left(\frac{-(p_z-q_{iz})}{\sqrt{(p_x-q_{ix})^2+(p_y-q_{iy})^2}}\right), \tag{24}$$

$$\xi_0 = \text{atan}\left(\frac{p_z-q_{0z}}{\sqrt{(p_x-q_{0x})^2+(p_y-q_{0y})^2}}\right), \tag{25}$$

$$\tau_i = \frac{\|\mathbf{p}-\mathbf{q}_i\|}{c}-\delta_t, \tag{26}$$

$$f_{d_0} = \mathbf{v}^{\mathrm{T}}\mathbf{u}_0\frac{f_c^g}{c}, \tag{27}$$

$$f_{d_i} = (\mathbf{v}-\mathbf{v}_i)^{\mathrm{T}}\mathbf{u}_i\frac{f_c^s}{c},\ i>0 \tag{28}$$

where c is the speed-of-light, $\mathbf{v}_i$ is the velocity vector of the i-th satellite, f_c^g and f_c^s are the carrier frequency used in the 5G and satellite navigation systems and

$$\mathbf{u}_i \triangleq \begin{bmatrix}u_{0x}\\u_{0y}\\u_{0z}\end{bmatrix} = -\frac{\mathbf{p}-\mathbf{q}_i}{\|\mathbf{p}-\mathbf{q}_i\|}. \tag{29}$$

A. 5G positioning EFIM

In order to derive the EFIM for 5G positioning, we consider an orthogonal frequency-division multiplexing (OFDM) waveform with N_{FFT} subcarriers and Δ_f subcarrier spacing. In the frequency domain the expression of the received signal, at the n-th subcarrier and at m-th beamformer is given by

$$u_{0m,n}=\sqrt{\frac{P_g}{N_{\text{FFT}}}}a_0\, g_{d,n}\, g_{f_n}\, g_{r,m}\, \boldsymbol{g}_t^{\mathrm{H}}\mathbf{x}_n+\mathbf{w}_m^{\mathrm{H}}\mathbf{n}_n, \tag{30}$$

where $g_{d,n}\triangleq e^{-j2\pi n\Delta_f}$, $g_{f_n}\triangleq e^{j2\pi f_{d_0}T_{sym}}$, $g_{r,m}\triangleq \mathbf{w}_m^{\mathrm{H}}\mathbf{a}_r(\tilde{\theta}_0,\tilde{\psi}_0)$, $\boldsymbol{g}_t\triangleq\mathbf{F}^{\mathrm{H}}\mathbf{a}_t(\phi_0,\xi_0)$ and $\tilde{\theta}_0,\tilde{\phi}_0$ refers to the observed angle-of-arrival at the UE, which can be obtained from the identity

$$\boldsymbol{\pi}(\tilde{\theta}_0,\tilde{\psi}_0)=\boldsymbol{\Gamma}(\alpha)^{\mathrm{T}}\boldsymbol{\pi}(\theta_0,\psi_0)=\boldsymbol{\pi}(\theta_0-\alpha,\psi_0). \tag{31}$$

The terms in (20) can be obtained from the block-matrix partion of

$$\mathbf{J}_{0m}=\mathbf{T}^{\mathrm{T}}\left(\sum_{n=1}^{N_{\text{FFT}}}\tilde{\mathbf{J}}_{0m,n}\right)\mathbf{T}, \tag{32}$$

where $\tilde{\mathbf{J}}_{0m,n}$ is the FIM for the physical-channel parameters $\tilde{\boldsymbol{\eta}}_g\triangleq[\tau_0,\tilde{\theta}_0,\tilde{\psi}_0,\phi_0,\xi_0,\Re(a_0),\Im(a_0),f_{d0}]^{\mathrm{T}}$ and $\mathbf{T}$ is given by

$$[\mathbf{T}]_{ij}=\frac{\partial\tilde{\eta}_{g,i}}{\partial\eta_j}, \tag{33}$$

in which the non-zero elements are given by

$$\frac{\partial\tilde{\theta}_0}{\partial\mathbf{p}}=\frac{d}{d_{xy}^2}\left[u_{0y},-u_{0x},0\right], \tag{34}$$

$$\frac{\partial\psi_0}{\partial\mathbf{p}}=\frac{1}{d_{xy}}\left[u_{0x}u_{0z},u_{0y}u_{0z},-d_{xy}^2/d^2\right], \tag{35}$$

$$\frac{\partial\tilde{\phi}_0}{\partial\mathbf{p}}=\frac{d}{d_{xy}^2}\left[u_{0y},-u_{0x},0\right], \tag{36}$$

$$\frac{\partial\xi_0}{\partial\mathbf{p}}=-\frac{1}{d_{xy}}\left[u_{0x}u_{0z},u_{0y}u_{0z},-d_{xy}^2/d^2\right], \tag{37}$$

$$\frac{\partial\tau_0}{\partial\mathbf{p}}=-\frac{\mathbf{u}_0^{\mathrm{T}}}{c}, \tag{38}$$

$$\frac{\partial f_{d_0}}{\partial\mathbf{p}}=\frac{f_c}{cd}(\mathbf{v}^{\mathrm{T}}\mathbf{u}_0-\mathbf{v})\mathbf{u}_0^{\mathrm{T}}, \tag{39}$$

and $\frac{\partial\tau_0}{\partial\delta_t}=1$, $\frac{\partial\tilde{\theta}_0}{\partial\alpha}=-1$, $\frac{\partial\Im\{a_0\}}{\partial\Im\{a_0\}}=1$, $\frac{\partial\Re\{a_0\}}{\partial\Re\{a_0\}}=1$, $d=\|\mathbf{p}-\mathbf{q}_0\|$, $d_{xy}=\sqrt{(p_x-q_{0x})^2+(p_y-q_{0y})^2}$.

Finally, the FIM $\mathbf{J}_{0m,n}\in\mathbb{R}^{8\times8}$ can be obtained by computing

$$\mathbf{J}_{0m,n}=\gamma_g\mathbb{E}_{x_n}\left\{\Re\left(\nabla_{\tilde{\boldsymbol{\eta}}_g}^{\mathrm{H}}u_{nm}\nabla_{\tilde{\boldsymbol{\eta}}_g}u_{nm}\right)\right\}, \tag{40}$$

where $\gamma_g=\frac{P_g}{N_0N_{\text{FFT}}\Delta_f}$, $u_{nm}=a_0\, g_{d,n}\, g_{f_n}\, g_{r,m}\, \boldsymbol{g}_t^{\mathrm{H}}\mathbf{x}_n$.

B. GNSS positioning EFIM

We focus on a Global Positioning System (GPS) technology with a carrier frequency f_c^s with $N_c=1023$ chips of duration $T_c=1/N_c$ ms, *i.e.*,

$$x_i(t)=\sqrt{P_{s_i}}\sum_{n=1}^{N_c}b_{in}\text{rect}_{T_c}(t-nT_c)e^{j2\pi f_c^s t}, \tag{41}$$

where $\text{rect}_{T_c}(t)$ is the rectangular pulse of unitary amplitude and duration T_c, P_{s_i} is the average transmission power and $\mathbf{b}_i\triangleq[b_{i1},\cdots,b_{iN_c}]$ is the code sequence transmitted by the i-th satellite. It is assumed $\mathbf{b}_i^{\mathrm{T}}\mathbf{b}_q=0$, $\forall i\neq q$.

Using equation (41) in (9) and by leveraging the orthogonality of the code sequences into the calculation of the EFIM, we compute $\mathbf{J}_s^e$ as in (15) where the matrices $\mathbf{J}_{s_i,\eta}$, $\mathbf{J}_{s,a_i}$ and $\mathbf{J}_{s,\eta a_i}^{\mathrm{T}}$ are obtained from the block-partition of

$$\mathbf{J}_{s_i}=\mathbf{T}_{s_i}^{\mathrm{T}}\tilde{\mathbf{J}}_{s_i}\mathbf{T}_{s_i}, \tag{42}$$

with $\tilde{\mathbf{J}}_{s_i}=\mathbb{E}\left\{\Re\left(\nabla_{\tilde{\boldsymbol{\eta}}_{s_i}}^{\mathrm{H}}u_{s_i}\nabla_{\tilde{\boldsymbol{\eta}}_{s_i}}u_{s_i}\right)\right\}$, $\tilde{\boldsymbol{\eta}}_{s_i}\triangleq[\tilde{\theta}_i,\tilde{\psi}_i,\tau_i,f_{di},\Re(a_i),\Im(a_i)]^{\mathrm{T}}$ and $\mathbf{T}_{s_i}$

$$[\mathbf{T}_{s_i}]_{qj}=\frac{\partial\tilde{\eta}_{s_i,q}}{\partial\eta_j}. \tag{43}$$

IV. Simulation results

The objective of this section is to evaluate the performance of an hybrid 5G-GNSS positioning system and compare it to 5G and GNSS stand-alone solutions. In this regard, we consider a 5G-mmW at 30 GHz, subcarrier spacing 60 kHz, transmission bandwidth 60 MHz, QPSK modulation and a GPS-based satellite positioning. Further details are in the sequel. UE: location coordinate $[0,0,0]^{\mathrm{T}}$ m, 5G uniform rectangular array (URA) 4×4 in the zy-plane, GPS receiver with URA 2×2 in the xy-plane, Discrete Fourier Transform (DFT) analog beam-codebook and sequential single beam-scanning. gNB: location coordinate $[-20,20,25]^{\mathrm{T}}$ m, 5G URA 8×8 in the zy-plane, DFT analog codebook and sequential single beam-scanning. Finally, GPS: observation time $T_s=20$ ms, bandwidth $B=4/T_c$, carrier frequency 1575.42 MHz and radius, azimuth and elevation directions of the satellites' locations

$$\boldsymbol{\varrho}_s = [2.19, 2.34, 2.47, 2.18, 2.45]\times 1\mathrm{e}5\,\mathrm{km}, \quad (44)$$

$$\boldsymbol{\theta}_s = [288.9, 215.2, 87.9, 295.4, 123.5]\,\mathrm{deg}, \quad (45)$$

$$\boldsymbol{\psi}_s = [46.9, 24.5, 29.1, 32.1, 71.5]\,\mathrm{deg}. \quad (46)$$

The first result is shown in Figure 2 where the x and y axis refer to the achieved localization error by GNSS and 5G standalone. More specifically, for 5G, we assume that UE is perfectly synchronized with gNB and the error is obtained by varying the SNR_0 ($i.e.$ the signal-to-noise ratio of the 5G signal without beamforming gain). For the GNSS, we assume that UE's clock-bias is non-zero and the performance depends on the carrier-to-noise C/N_0 (signal power to noise spectral density, typically used in GNSS). The contour plot corresponds to the hybrid 5G-GNSS solution obtained for all pairs $(\mathrm{SNR}_0, C/N_0)$ used for calculating 5G and GNSS bounds. It can be noticed that the hybrid method provides always a lower error than that obtained by a 5G or GNSS systems. Therefore, if one of the systems fails in terms of accuracy, the performance of an hybrid system takes advantage of the best between the two.

Next, we evaluate a more realistic scenario where UE clock is not synchronized with either 5G or GNSS, and the clock bias is unknown. Figures 3 and 4 show the localization error achieved with 5 and 3 satellites, respectively. The black-solid line corresponds to the performance of the GNSS, whereas the colored dash and solid lines indicate 5G system with perfectly synchronized UE's clock and hybrid 5G-GNSS system with unknown UE's clock bias, respectively.

In both simulations, it can be noticed that the proposed 5G-GNSS method is always more accurate than the GPS[4] but, only after a certain carrier-to-noise value, it is better than a perfectly synchronized 5G system. In other words, this study indicates that exists a certain value of the carrier-to-noise signal, beyond which a practical 5G positioning can benefit of the interaction

[4]GPS positioning with three satellites is theoretically feasible by using an antenna array and, especially observing the Doppler shifts at the receiver since the dependence of both the AoA and Doppler with the position is exploited. However, errors are very large for realistic C/N_0.

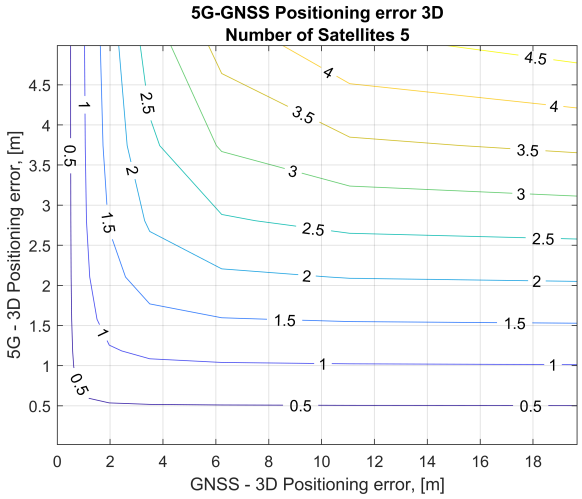

Fig. 2. Contour plot of the hybrid system with perfectly synchronized UE.

with GNSS to improve accuracy. However, this value varies with the number of satellites by comparing Figures 3 and 4.

Figure 5 illustrates the estimation error of the UE clock-bias. It can be noticed that no performance is shown for the stand-alone 5G system as the UE clock-bias is not identifiable with mere LOS measurements. However, both GNSS and hybrid 5G-GNSS can provide an estimate of the bias that improves with carrier-to-noise. The benefits of a joint processing of 5G and GNSS observables are clearly remarked by the lower error achieved by this solution, which is more accentuated in the low carrier-to-noise regime and less at unrealisticly high carrier-to-noise ratios. Comparing this result with the location error shown in Figure 4, a tight correlation can be identified which, for instance, can be exploited for a mutual performance improvement by using side information of location or synchronization.

Next, in Figure 6 the estimation error of the UE's rotation is provided. In this case, the performance is plotted as a function of the 5G Signal-to-Noise Ratio (SNR) as we are interested to a direct comparison of to the orientation error with 5G. Again, the advantage of the hybrid positioning is proved as the achievable error is lower than the best of the two solutions.

In contrast to the location error, the 5G-GNSS performance lines do not intersect the others. This indicates that there is no minimum carrier-to-noise requirement, since the hybrid solution always improves the orientation estimation.

Finally, as an example, let us mention that a specific positioning requirement, $e.g.$ 50 cm, can be achieved by either with a very good GNSS configuration (5 satellites and $C/N_0 = 57$ dBHz) or by a hybrid solution with at least 3 satellites with $C/N_0 = 60$ dBHz, 5G SNR -14 dB. By increasing the 5G SNR, weaker requirements on GNSS signals can be imposed.

V. Conclusion

In this paper we studied the fundamental limits of 5G-GNSS solution for positioning, orientation and UE's clock-

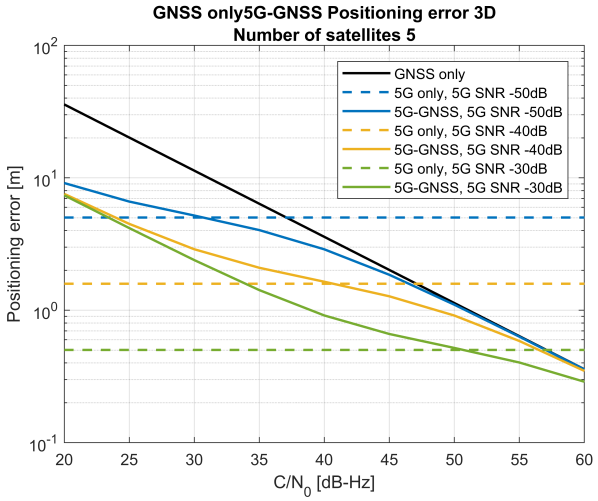

Fig. 3. Behaviour of a 5G-GNSS position error as a function of the GNSS carrier-to-noise and using the GNSS observables from 5 satellites.

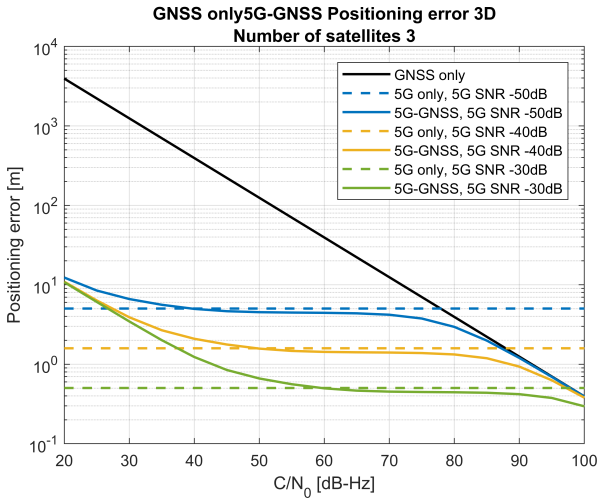

Fig. 4. Behaviour of a 5G-GNSS position error as a function of the GNSS carrier-to-noise and using the GNSS observables from 3 satellites.

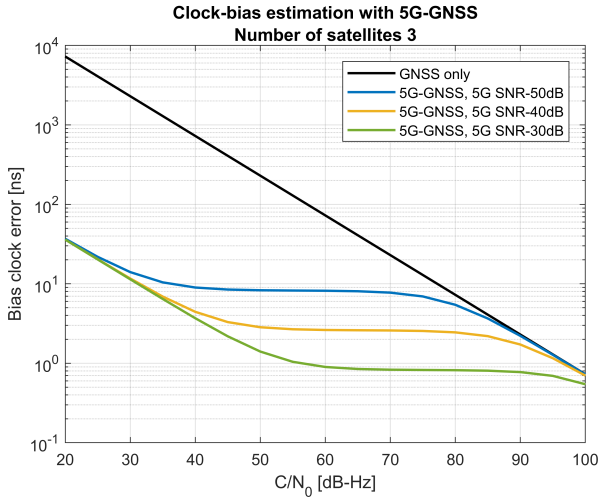

Fig. 5. Behaviour of a clock-bias error as a function of the GNSS carrier-to-noise and using the GNSS observables from 3 satellites.

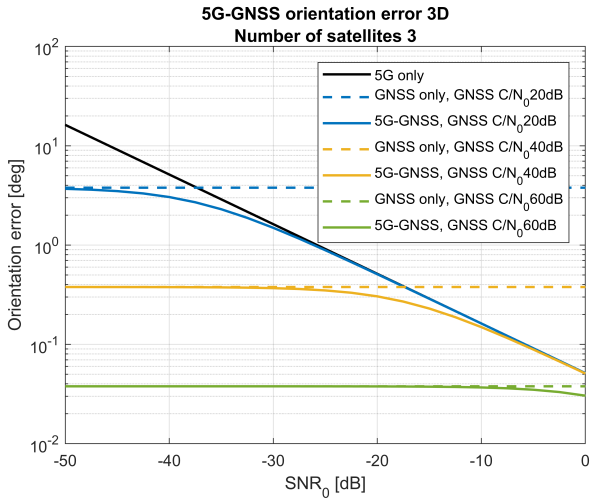

Fig. 6. Behaviour of a UE orientation error as a function of the 5G SNR (without beamforming) and using the GNSS observables from 3 satellites.

bias estimation. It was found that, with a tight coupling of the observables, GNSS benefits from 5G to improve localization accuracy and reduce the number of connected satellites. On the other hand, 5G takes advantage of a GNSS system to improve gNB-UE synchronization issues as well as to achieve better localization and orientation accuracy in the low SNR regime. The Doppler was useful to increase the rank of the FIM.

ACKNOWLEDGMENTS

This work was supported, in part, by the Academy of Finland projects 6Genesis Flagship (grant 318927), Fundamental of Simultaneous Localization and Communications (grant 298781), and Positioning-aided Reliably-connected Industrial Systems with Mobile mmWave Access (PRISMA), by the EU H2020 project 5GCAR, and the VINNOVA COPPLAR project, funded under Strategic Vehicle Research and Innovation Grant No. 2015-04849 and R+D Project of Spanish Ministry of Economy and Competitiveness under Grant TEC2017-89925-R.

REFERENCES

[1] H. Wymeersch, G. Seco-Granados, G. Destino, D. Dardari, and F. Tufvesson, "5 mmwave positioning for vehicular networks," *IEEE Trans. Wireless Commun.*

[2] E. S. Lohan, M. Koivisto, O. Galinina, S. Andreev, A. Tolli, G. Destino, M. Costa, K. Leppanen, Y. Koucheryavy, and M. Valkama, "Benefits of Positioning-Aided Communication Technology in High-Frequency Industrial IoT," *IEEE Commun. Mag.*, pp. 1–7, 2018.

[3] P. J. G. Teunissen and O. Montenbruck, *Handbook of Global Navigation Satellite Systems*. Springer, 2017.

[4] A. Shahmansoori, G. E. Garcia, G. Destino, G. Seco-Granados, and H. Wymeersch, "position and orientation estimation through millimeter-wave MIMO in 5G systems," *IEEE Transactions on Wireless Communications*.

[5] J. del Peral-Rosado, J. Saloranta, G. Destino, J. Lòpez-Salcedo, and G. Seco-Granados, "Methodology for Simulating 5G and GNSS High-Accuracy Positioning," *Sensor*, vol. 18, no. 10, 2018.

[6] S. M. Kay, *Fundamentals of Statistical Signal Processing: Estimation Theory*. Upper Saddle River, NJ, USA: Prentice-Hall, Inc., 1993.